

# Bystander Effect of Sonodynamic Therapy in the presence of Gold Nanoparticles: An in-vitro study

A. Shanei<sup>1</sup>, R. Kamran Samani<sup>2</sup>, H. Akbari-Zadeh<sup>3,4</sup>, M. Rezaei<sup>1\*</sup>, M. Kazemi<sup>5</sup>

<sup>1</sup>Department of Medical Physics, School of Medicine, Isfahan University of Medical Sciences, Isfahan, Iran

<sup>2</sup>Department of Medical Physics and Radiology, School of Allied Medical Sciences, Shahrekord University of Medical Sciences, Shahrekord, Iran

<sup>3</sup>Department of Medical Physics, Faculty of Medicine, Mashhad University of Medical Sciences, Mashhad, Iran

<sup>4</sup>Student Research Committee, Mashhad University of Medical Sciences, Mashhad, Iran

<sup>5</sup>Department of Genetics and Molecular Biology, School of Medicine, Isfahan University of Medical Sciences, Isfahan, Iran

## ► Original article

## ABSTRACT

### \*Corresponding author:

Masumeh Rezaei, MSc.,

### E-mail:

[masumrezaei@yahoo.com](mailto:masumrezaei@yahoo.com)

Received: October 2021

Final revised: June 2022

Accepted: October 2022

Int. J. Radiat. Res., July 2023;  
21(3): 391-398

DOI: 10.52547/ijrr.21.3.6

**Background:** Bystander (B.s) effect can influence non-irradiated cells and affect the desired effect in cancer treatment. This study was conducted to assess this effect on simultaneous administration of ultrasound (US) and Gold nanoparticles as a sonodynamic therapy (SDT) which is an important newly stimuli-responsive method in cancer treatment. **Materials and Methods:** Firstly, the appropriate concentration of Gold nanoparticles (GNPs) and US intensity for SDT on melanoma cancer cells (A375) were evaluated. After treatments, the target cell culture was transferred to the bystander cells and the induced bystander effects including cell viability, apoptosis, expression of P53 (a promoter of apoptosis gene) and HO-1 (an inhibitor of apoptosis gene) were examined. **Results:** According to the MTT results, 50 µg/ml concentration of GNPs and 1.5 W/cm<sup>2</sup> intensity of US wave were selected. Our results revealed that SDT induced B.s effect can alter the cell viability and apoptosis up to 20% and 51.61%, respectively. Moreover, a 2.9-fold increase in p53 gene expression and a decrease in HO-1 gene expression to 0.181-fold in comparison to the control groups were observed. **Conclusions:** These results confirmed that B.s effect of sonodynamic can reduce the cancerous cell viability. Our finding showed that this treatment can potentially be an alternative to traditional treatment modalities.

**Keywords:** Bystander effect, sonodynamic therapy, gold nanoparticles, apoptosis, p53 & HO-1 genes.

## INTRODUCTION

Cancer is a global disease that affects life of many people in the world. Standard cancer treatment options include chemotherapy, radiotherapy and immunotherapy <sup>(1)</sup>. Unlike traditional therapies, stimuli-responsive therapies can be controlled to increase targeted responses and decrease side effects <sup>(2)</sup>. Sonodynamic therapy (SDT) is one of them that combines ultrasound (US) wave with chemotherapy drugs called as sonosensitizers <sup>(3)</sup>. This treatment leads to generation of reactive oxygen species (ROS) such as hydrogen peroxide (H<sub>2</sub>O<sub>2</sub>), hydroxyl radicals (OH), and hydroperoxyl radicals which disrupts cancerous cellular function and damages to it <sup>(4)</sup>. Deeply penetration of US waves in SDT is a major therapeutic advantage over other stimulus-responsive treatment for the destruction of deeper or larger tumours <sup>(5)</sup>.

In recent years, diagnosis and treatment of cancers have been revolutionized with the advent of various nanoparticles <sup>(6,7)</sup>. The unique properties of nanoparticles compared to chemotherapeutic agents, as well as their synergistic effects when combined

with US waves, make them good candidates to substitute chemotherapeutic agents <sup>(8)</sup>. Gold nanoparticles (GNPs) with low toxicity, a unique physical and chemical properties and good biocompatibility is an excellent option for SDT <sup>(3,8,9)</sup>.

Despite researchers' best efforts to improve the quality of cancer treatment, clinicians often couldn't be achieving the desired results. This could be due to existence of secondary radiation effects such as bystander (B.s) phenomenon <sup>(10)</sup>. It is accepted that direct collision of radiation with a cell can damage its DNA and lead to biological effects. Nevertheless, they are not the only radiation effects, and non-targeted cells can also respond to the radiation <sup>(11)</sup>. Some studies have been shown that this phenomenon reduces cancerous cell survival by affecting their DNA and signaling molecules <sup>(12)</sup>. However, in other some studies known that the B.s effects have negative effect on cancer treatment due to creating cell death resistant, sustaining proliferative signaling, evading growth suppressors, avoiding immune destruction tumor-promoting inflammation and genome instability and mutation <sup>(10,13,14)</sup>. The existence of these effects indicates that the occurrence of any

biological effect is not solely related to the number of irradiated cells <sup>(15)</sup>. Therefore, studying and considering B.s effect in different fields such as protection, radiotherapy, and side effects in normal tissues seems to be necessary <sup>(16,11)</sup>.

The B.s effect has been studied for different cancer treatment such as ionizing radiation, photodynamic treatment <sup>(17)</sup>, chemotherapeutic drugs <sup>(18)</sup>, and radiofrequency waves <sup>(19)</sup> but there are no studies on B.s effect in SDT as an important stimulus-responsive treatment. Therefore, this study was performed to investigate the B.s effects on melanoma cancer cells when treated with SDT.

## MATERIALS AND METHODS

### Experimental design

In this study, we used the target cell growth medium transfer technique to induce the B.s effect in non-irradiated cells <sup>(20)</sup>. At the first step, we tried to find the proper component of GNPs concentration and US intensity for SDT on A375 cells using MTT assay.

After obtaining the appropriate combination of US waves with GNPs, target cells were treated in different groups including US, GNPs, and US+GNPs and their cell culture medium was harvested and added to the non-irradiated cells. Finally, the viability of all B.s groups was measured with MTT assay, and for each group that showed change in cell viability, the apoptosis, and gens expressions (*P53* and *HO-1* genes) assays were performed. The outline of the experiment, intervention, and the time interval between them are shown in figure 1.

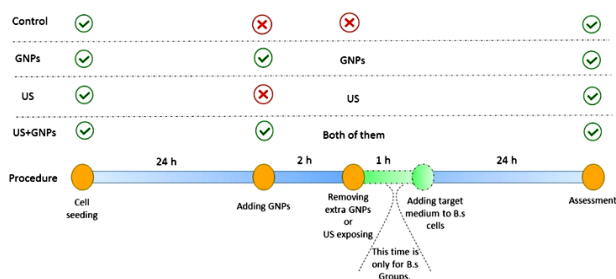


**Figure 1.** The general schematic of the experiment, intervention, and the time interval between them.

### Cell culture

A375 (human melanoma) cell line was purchased from Pasteur Institute in Tehran, Iran. A375 was cultured in RPMI 1640 medium (Roswell Park Memorial Institute 1640, Gibco, Germany) containing 10% Fetal Bovine Serum (FBS, Gibco, Germany), streptomycin (1 µg/ml, Biosera, France) and penicillin (100 units/ml, Biosera, France) and it was incubated at 37 °C in an atmosphere with 5% CO<sub>2</sub>.

### Synthesis and characterization of GNPs

The synthesis of GNPs was done according to the

same method which described in our previous study <sup>(21)</sup>. At first, 50 mL of 0.01% HAuCl<sub>4</sub> solution was heated to boiling temperature while being stirred in a 100 mL round bottom flask. Then, 400 µL of 1% trisodium citrate solution was added. The size and morphology of GNPs were determined using Transmission Electron Microscopy (TEM, Philips em208s, 100kV, Netherlands), and particle size distribution was evaluated by using Dynamic Light Scattering (DLS, Nanoparticle Analyzer, SZ-100, Horiba Company, Japan).

### Evaluation of GNPs cytotoxicity in target cells

To determine the optimal concentration of GNPs, the cells were seeded in a 96 microwell plate (Zhejiang Sorfa Life Science Research Co., Ltd., Huzhou, China) at a density of  $12 \times 10^3 \frac{\text{cell}}{\text{well}}$  and then they were incubated for 24 h. Afterwards, the culture medium of the cells was replaced with media containing GNPs at different concentrations (0.5, 1, 10, 20, 30 to 100 µg/ml) and were incubated for 2 h. Then, the culture medium was removed and the cells were washed twice with PBS. The cells were incubated with a fresh medium for 24 h. Finally, the effect of GNPs on cell viability was measured by MTT assay.

### Assessment of cellular internalization

The amount of internalized GNPs to the melanoma cells was determined using the ICP-OES assay. The A375 cells were seeded at a density of  $1 \times 10^6$  cells/well in a 6-well plate (Zhejiang Sorfa Life Science Research Co., Ltd., Huzhou, China) and were incubated overnight. Afterwards, the cell culture medium was replaced by a fresh medium containing optimum concentrations of GNPs. After 2 h, the culture medium was removed and the cells were washed three times using PBS. After that, the cells were detached by trypsin, counted and collected by centrifugation. Then, they were lysed in 3 mL of a solution containing 3:1 (v/v) hydrochloric acid (12.5 M) and nitric acid (5 M)). The amount of GNPs uptake per cell was measured using ICP-OES (Varian Vista-Pro, Australia).

### US generator system and exposure set up

The US system used in this study was a 1 MHz therapeutic unit in a continuous mode (215A; a coproduct of Novin Medical Engineering Co, Tehran, Iran; and EMS Co, Reading, Berkshire, England) with a 29.8 mm diameter probe and 7.0 cm<sup>2</sup> effective radiation area.

For US exposure, the unfocused transducer was fixed in a hole at the bottom of the water tank; then the 12-well plate (Zhejiang Sorfa Life Science Research Co., Ltd., Huzhou, China) was placed in far-field (out of the near field) for uniform intensity exposure so that the distance between cells adhered to the floor of the plate and the US transducer was 15

cm as shown in figure 2.

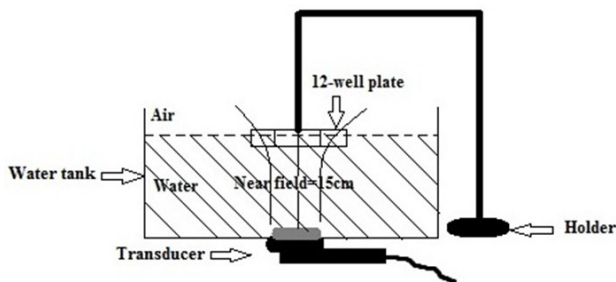


**Figure 2.** General schematic of ultrasound exposure setup for uniform irradiation.

### US exposure of target cells with and without GNPs

The cells were cultured in 12-well plates ( $5 \times 10^4$  cell/well) and were incubated for 24 h. In the group of GNPs with the US, the target cells were treated with nanoparticles for 2 h. After this time, the cell culture was completely removed and washed three times with PBS. Then, they were exposed to 1 MHz US at 0.5, 1, 1.5, and 2 W/cm<sup>2</sup> intensities (I<sub>SATA</sub>) for 5 min.

### Induction of the bystander effect

After target cells treatment in different groups, the target cells culture medium was transferred to B.s cells to evaluate their effects on them. For this reason, one hour after the US exposure, the cell culture medium was collected and passed through a filter (0.22 µm) and transferred to the specified B.s cell plates. The B.s cells were incubated for 24 h after receiving the target group culture medium. Then, the cell viability was measured using MTT assay, and each group that showed a B.s effect was further examined by apoptosis and Real-time PCR assays.

### MTT assay

The MTT test (5 mg/mL) (Sigma, St. Louis, MO, USA) was performed to investigate the percentage of cell viability. In the MTT assay, the mitochondria of live cells were colored and analyzed by a microwell plate reader to calculate the cell viability rate. For this reason, the cell culture media of each well were removed, the cells were washed and a mixture of 100 µl RPMI with 10 µl of MTT solution (5 mg/mL) was added to them. After that, the cells were incubated for 4 hours. Then, the MTT solution was removed, and 50 µl of DMSO (Sigma, USA) was added to each well and was incubated again for 15 min. Finally, optical densities (ODs) of these wells were measured at 570 nm by a microwell plate reader (Bio-RAD 680, USA). The cell viability was determined using eq. 1:

$$\text{Cell viability} = \frac{\text{OD}_{\text{treated}}}{\text{OD}_{\text{control}}} \times 100 \quad (1)$$

### Apoptosis in B.s cells

Apoptosis was detected by the eBioscience™ Annexin V Apoptosis Detection Kit II (Invitrogen, USA). After B.s cell treatments, the culture medium of

each well was collected. The cells were washed once with cold and fresh PBS, then 100 µl of buffer (1x) with 2 µl of annexin-V and 2 µl of propidium iodide (PI) were added to the cells and were incubated for 20 min at room temperature in the dark. Finally, 300 microliters of buffer were added and 10,000 cells for each sample were recorded on a flow cytometer.

### RNA extraction and Real-time PCR

Total RNA was isolated from cells using BioFACT Total RNA prep Kit (BioFACT, Korea) according to the manufacturer's instructions. Isolated RNA quantity and quality were determined by measuring absorbance at 260 nm and 280 nm with a 2000 nanodrop (Thermo Scientific, USA). The RNA samples were treated with DNase I (Thermo Scientific, USA) to avoid potential contamination with genomic DNA. Five micrograms of total RNA were used to synthesize cDNA using BioFACT 2X Onestep Real-time PCR Master Mix kit (BioFACT, Korea) and oligo (dT) primers. The primers for all assayed genes were used according to Table 1. The Real-time polymerase chain reaction was performed using BioFACT 2X Real-time PCR Master Mix (High ROX) containing SYBR Green (BioFACT, Korea) and the StepOne Plus™ Real-time PCR detection system (Applied Biosystems, Foster City, CA, USA). GAPDH was used as an endogenous control, and the expression level of each target gene was calculated as  $2^{-\Delta\Delta C_t}$ .

**Table 1.** Sequences (5' to 3') of the primers used in the detection of different genes.

Gene	Forward	Reverse	Primer Length
GAPDH	TGGTATCGTG-GAAGGACTC	AG-TAGAGGCAGGGATGATG	130bp
P53	TCTGACTGTACCAC-CATCCACTA	CAAAACGCAC-CTCAAAGC	146bp
HO-1	CAACAAAGTGCAA-GATTCTG	AAAGCCCTACAG-CAACTG	134bp

### Data analysis

Statistical calculations were performed with the GraphPad Prism (version 7.01.; GraphPad Software, La Jolla, CA, USA). The Kolmogorov-Smirnov normality test indicated that all data had normal distribution. Therefore, one-way ANOVA, Tukey's multiple comparisons and Dunnett's tests were utilized at  $P < 0.05$ . Each experiment was repeated at least three times. All data are expressed as mean  $\pm$  SD in the figures.

## RESULTS

### Characterization and cytotoxicity of GNPs

At the first step, we synthesised and characterized the GNPs. The result of GNPs characterization is shown in figure 3. DLS results demonstrated that

GNPs are uniformly dispersed with a particle size of  $\sim 13$  nm (figure 3(A)), and TEM showed GNPs have a spherical shape (figure 3(B)).

According to figure 4 which show the result of GNPs cytotoxicity, the effect of different concentrations of GNPs on melanoma cancer cells indicated that concentrations below 50  $\mu\text{g/ml}$  have no significant differences from the control group ( $P>0.05$ ) and all of them almost show the same effects. In addition, the cell viability was dramatically reduced at concentrations above 50  $\mu\text{g/ml}$ . For this reason, we used this concentration (50  $\mu\text{g/ml}$ ) for subsequent experiments.

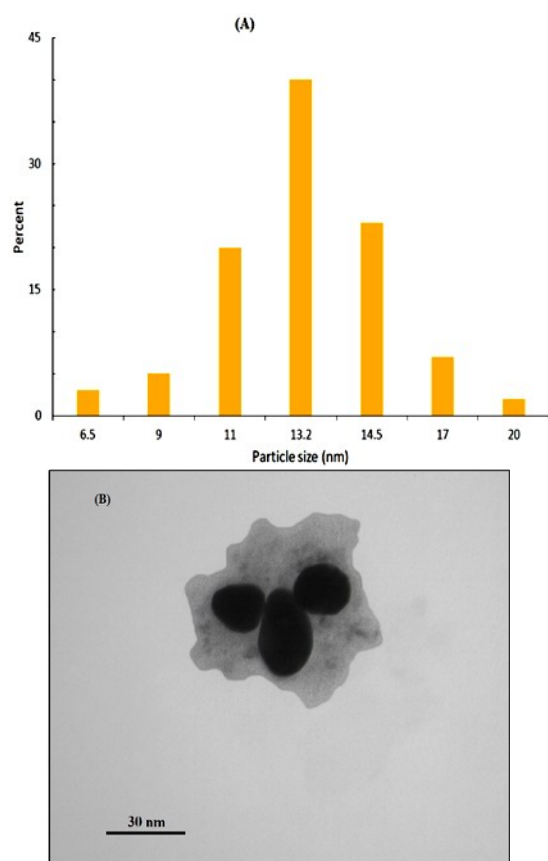


**Figure 3.** Characterization of the GNPs with (A) DLS and (B) TEM image.

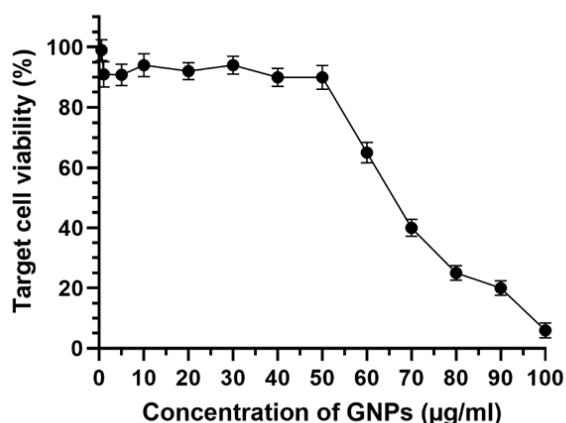


**Figure 4.** Percentage viability of the targeted cells were treated with different concentrations of GNPs for 2 h followed by 24 h incubation. GNPs: gold nanoparticles.

The ICP-OES results showed that the GNPs have significantly penetrated the A375 cells during 2 h (3.8  $\mu\text{g}/10^6$  cells).

#### **Effect of different intensities of the US with and without GNPs (50 $\mu\text{g/ml}$ ) on the targeted cells**

After selecting the concentration of 50  $\mu\text{g/ml}$  of GNPs for our study, we evaluated the effect of different intensities of the US waves with and without presence of GNPs on the target cell. The figure 5 represent these result. According to figure 5, when US intensity (with or without GNPs) was increased, cell viability in target groups was reduced. There are significant differences in target cell viability between 1  $\text{W}/\text{cm}^2$  (80%), 1.5  $\text{W}/\text{cm}^2$  (74%) and 2  $\text{W}/\text{cm}^2$  (60%) US intensities with control group ( $P<0.05$ ).

Moreover, adding the GNPs on studied intensities reduces their target cell viability by 2%, 12%, and 16% more. Among them, combination of GNPs with 1.5 and 2  $\text{W}/\text{cm}^2$  showed significant differences from US-only group ( $P<0.05$ ).

Considering that the combination of GNPs (50  $\mu\text{g/ml}$ ) with 1.5  $\text{W}/\text{cm}^2$  US waves showed significant differences with US-only and control groups, we chose this combination as the first candidate to evaluate the B.s effect on melanoma cells.

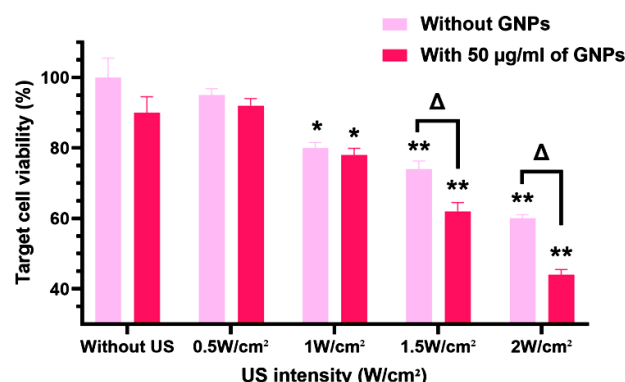


**Figure 5.** Cell viability in target cells with and without GNPs after different US intensities measured by MTT assay after 24 h. The \* indicated the groups that have significant differences (\* $p<0.05$  and \*\* $p<0.01$ ) with a control group, and  $\Delta$  indicated the combination group that has significant differences from the US-only group ( $p<0.05$ ). US= ultrasound, GNPs: gold nanoparticles.

#### **Effect of GNPs (50 $\mu\text{g/ml}$ ), US (1.5 $\text{W}/\text{cm}^2$ ), and their combination on B.s cells**

##### **MTT assay**

We first used the MTT assay to evaluate the effects of GNPs, US and their combination on B.s cells. The viability of B.s cells, which received the culture medium of target cells with GNPs-only, had no significant differences from non-targeted cells ( $P>0.05$ ). These results are shown in figure 6.

According figure 6, the viability of the B.s cells with or without GNPs (50  $\mu\text{g/ml}$ ) for 1.5  $\text{W}/\text{cm}^2$  US intensity shows a significant difference ( $P<0.05$ ) from the control group. In addition, MTT results indicated



that adding GNPs to US waves can reduce the viability of the B.s cells up to 20% which is 7% more than the US alone group, and both of them have significant differences together ( $P < 0.05$ ).

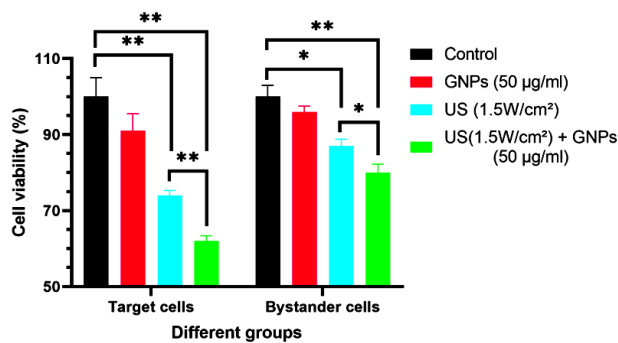


**Figure 6.** Percentage of cell viability in target and bystander groups at different conditions with MTT assay after 24 h (\* $p < 0.05$  and \*\* $p < 0.01$ ). US= ultrasound, GNPs: gold nanoparticles.

### Apoptosis assay

The figure 7 show the result of B.s cells flow cytometry in different group. In this figure, the lower and upper right quadrants show early and late apoptosis, respectively. The total percentage of apoptosis in B.s cells according to the flow cytometry is shown in figure 8. The percentages of apoptosis in the B.s groups after US ( $1.5 \text{ W/cm}^2$ ) exposure with or without  $50 \text{ µg/ml}$  GNPs are 51.61% and 34.01%, respectively. As shown in figure. 8, the percentage of apoptotic B.s cells which received the target cell culture in different conditions indicated that all groups have significant differences from each other ( $P < 0.05$ ).

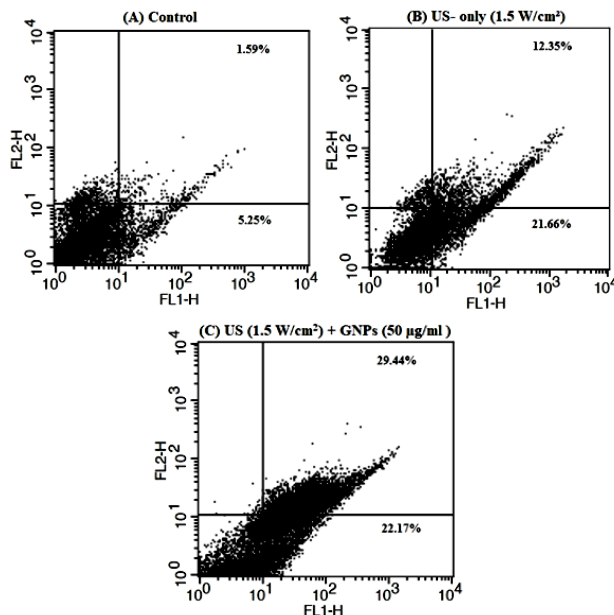


**Figure 7.** Contour diagrams of Annexin V/PI flow cytometry of A375 cells in the different Bystander groups: (A) control (B) only therapeutic US wave ( $1.5 \text{ W/cm}^2$ ) (C) therapeutic US ( $1.5 \text{ W/cm}^2$ ) with GNPs ( $50 \text{ µg/ml}$ ) pre-treatment. US= ultrasound, GNPs: gold nanoparticles.

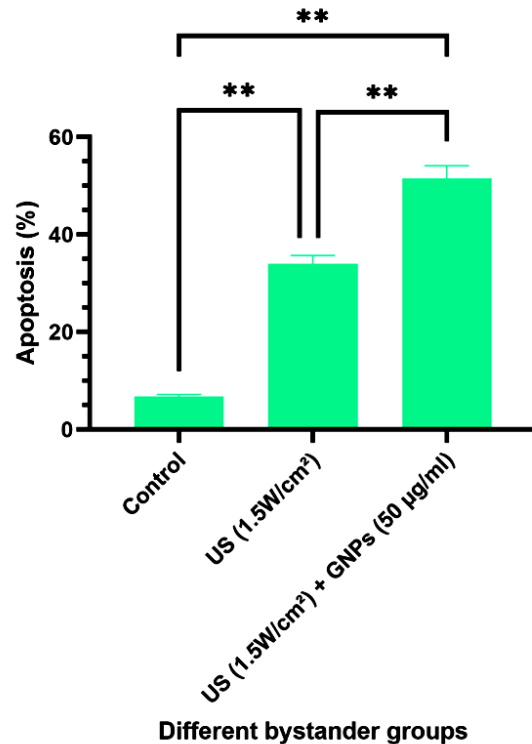


**Figure 8.** Percentage of apoptosis in Bystander groups after 24 h (\*\* $p < 0.001$ ). US= ultrasound, GNPs: gold nanoparticles.

### Expression of p53 and HO-1 genes in target and B.s cells

To confirm the previous results, the expression level of *p53* and *HO-1* genes in target and B.s cells were also examined. The Figure 9 represent this result. According to figure 9(A), the *p53* gene expression in US exposure without GNPs in target and B.s groups in comparison to the control group showed a 5.2 and 2.7-fold increase, respectively. In addition, the expression of *p53* in target and B.s groups in US exposure with GNPs had 6.36 and 2.9 fold increases ( $P < 0.001$ ).

Figure 9(B) illustrated a reduction in *HO-1* expression after US exposure without GNPs in target and B.s groups. The level of *HO-1* gene expression in these groups had 0.17 and 0.42 fold decreases. Moreover, in US exposure with GNPs, *HO-1* gene expression in target and B.s groups had 0.064 and 0.181 fold decreases, respectively. The reduction of gene expression in the target cells is higher than those of the B.s cells. In other words, the use of US ( $1.5 \text{ W/cm}^2$ ) wave with and without GNPs ( $50 \text{ µg/ml}$ ) had significant differences in genes expression in B.s groups ( $p < 0.05$ ).

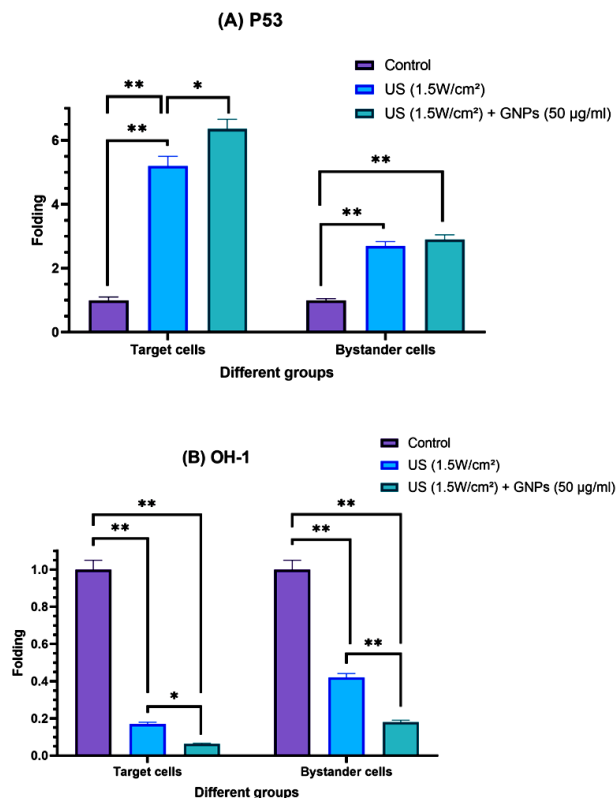


**Figure 9. (A)** Level of P53, and **(B)** HO-1, genes expression in target and bystander groups. (\* $p < 0.05$  and \*\* $p < 0.001$ )  
US= ultrasound, GNPs: gold nanoparticles.

## DISCUSSION

Considering that, it is necessary to know about the different biological effects of cancer treatment to make the right decision about their principle and proper use, this study was conducted to evaluate the B.s effect on melanoma cancer cells when treated with SDT. For this purpose, we first found the optimum concentration of GNPs, US intensity, and their combination effect on target cells, and then their B.s effect on the cells was evaluated.

Our results showed that the target cell viability is inversely related to the GNPs concentration and the US intensity (Figures 4 and 5). In addition, the concurrent administration of US and GNPs can cause synergistic effects. Therefore, adding GNPs with 50 µg/ml concentration to 1.5 W/cm<sup>2</sup> US intensity can reduce cell target viability by 38% (figure 5). This effect was observed in our pervious study on HeLa cells (22). Kosheleva *et al.* (8) reported that US waves with or without GNPs cause lung cancer cell death, but adding GNPs to the culture media before US exposure enhances the damage of target cells up to 30.7%. US waves can generate inertial cavitation inside a tumor region (23). Inertial cavitation process consists of nucleation, growth to near resonance size, and the collapse of bubbles (24, 25). The collapse of microbubbles is induced mechanical shock waves and produces high temperature and pressure focal

points (3, 25). These events lead to the formation of free radicals species and apoptotic initiators (23). According to previous studies, radical species including hydrogen peroxide (H<sub>2</sub>O<sub>2</sub>), hydroxyl radicals (OH), and hydroperoxyl radicals (HOO) that induced some chemical events were identified after cavitation (4). All of these events can cause cell damage and death (4, 23-25). Although the exact mechanism of the synergistic effect of GNPs in combination with US is not well known (26), however, the reduction of the threshold required for the cavitation production in US wave is one of the most important reason. In addition, Brazzale *et al.* (27) believed that GNPs have a high sonoluminescence absorption coefficient and the absorption of light generated in cavitation can lead to an increase rapidly their temperature and causes more ROS production.

After medium transfer technique for all groups (US, GNPs, US+GNPs) the MTT assay for bystander cells was performed. As expected, because the nanoparticles had no effect on the target cells, no effect was observed on the B.s cells (figure 6). This result was in agreement with the study of Rostami *et al.* that was done with a combination of nanoparticles and ionizing radiation (28).

The use of US wave can lead to B.s effect on the melanoma cancer cells, and adding GNPs to it can reduce the B.s cells viability to 83% compared to the control (figure 6). The results of flow cytometry confirmed our results of MTT assay (figure 7). The percentage of apoptosis in the B.s groups after 1.5 W/cm<sup>2</sup> US exposure with 50 µg/ml GNPs is 51.61% (figure 8). This result indicates that GNPs can increase the B.s effect on melanoma cancer cells.

Although the exact mechanism of the B.s effect is not completely discovered, the study on ionizing radiation indicated that oxidative stress plays a really important role in the generation, release and propagation of these B.s signals, which finally can alert cell function and biological effects (29). The interaction of DNA with ROS lead to creating different types of DNA oxidation. DNA oxidation as well as cell death through necrosis and apoptosis stimulate inflammatory responses and oxidative stress, causing further DNA damage in B.s cells (30, 31). Exosomes are microvesicles that can be secreted in normal and cancerous cells. These microvesicles can be as signals and affect cell function. The content of exosomes and its impact on other cells highly depend on the damaged cell type. Exosome release is increased in irradiated cells and they affect ROS production and DNA damage in B.s cells (30, 32). For these reasons and more detailed investigation and to prove our results, the transcription changes in target and B.s group cells were assessed using Real-time PCR and examined two *p53* and *HO-1* genes expressions as responses to the B.s effect.

The *p53* gene contributes to the DNA repair, cell

cycle regulation, and apoptosis. The most important effect of *p53* is arresting damaged cells in G1/S phase to extend G1 phase. This arrest gives the chance to cells for repairing their DNA damages and prevents the transmission of damaged gene to the daughter cells<sup>(14)</sup>. According to figure 9, the expression of *p53*, in target and B.s groups treated with 50 µg/ml GNPs and 1.5 W/cm<sup>2</sup> were 6.36 and 2.9 fold increase, respectively.

The results of the study that was conducted by Bohari *et al.* [33] in 2017 showed that a more than 5 fold increase level of *p53* gene expression in directly exposed MCF-7 cells after US. We also encountered the same effects in target cells. In their experiments with ionizing radiation on the HepG2 cell line, Olsson *et al.*<sup>(34)</sup> observed increased *p53* gene expression levels in B.s cells. Koturbash *et al.*<sup>(35)</sup> in 2008 investigated the B.s effects in a mouse model. They irradiated a part of the scalp of a mouse with ionizing radiation while covering the rest of the body with lead shields. Their results showed a significant increase in *p53* gene expression in the spleen cells as the B.s tissue.

Another gene which evaluated in this study was *HO-1*. *HO-1* is an antioxidant enzyme that exhibits significant anti-inflammatory and anti-apoptotic functions<sup>(36)</sup>. The level of *HO-1* expression in various types of cancer cells has been reported to be high, which may indicate that the increasing growth rate of cancer cells<sup>(37)</sup>. Therefore, in these cancers, *HO-1* inhibition or downregulation may lead to reduced tumor growth<sup>(38)</sup>. Halina *et al.* showed that *HO-1* overexpression increased tumor cell proliferation and improved angiogenic capability. In addition, *HO-1* causes cell resistance against oxidative stress. They claimed these events cause aggressive and metastasis nature of melanoma cancer both in vitro and *in-vivo*. Therefore, down-regulation of *HO-1* might be beneficial in the melanoma treatments, and may increase apoptosis in melanoma cells<sup>(39)</sup>.

According to figure 9, U.s with or without GNPs inhibits the expression of the *HO-1* gene in target cells. Moreover, *HO-1* expression in B.s cells that received the US exposed cell culture with or without GNPs was reduced. Increasing the apoptotic rate of B.s cells is in agreement with changes in *p53* and *HO-1* genes expressions. In the other words, the apoptosis in B.s cells may be correlated with increasing *p53* expression as a promoter of apoptosis and decreasing *HO-1* expression as an apoptosis inhibitor.

## CONCLUSION

Our result revealed that B.s effect of SDT can reduce the cancerous cell viability and this treatment is showing promise as a potentially vital alternative to traditional treatment modalities.

## ACKNOWLEDGEMENTS

This work was supported by the Medical Physics Department of Isfahan University of Medical Sciences, Isfahan, Iran.

**Funding:** No Funding.

**Conflict of interest:** All authors declare no conflicts of interest in this paper.

**Ethical consideration:** For this article no studies with human participants or animals were performed by any of the authors.

**Author Contributions:** A. Shanei: Supervision, Project administration, Funding acquisition. R. Kamran Samani: Writing original draf, Investigation & Calculation. H. Akbari-Zadeh: Writing original draf, Investigation & Calculation. M. Rezaei: Writing original draf, Investigation, Calculation, Data collection. M. Kazemi: Review & editing.

## REFERENCES

1. Miller KD, Siegel RL, Lin CC, *et al.* (2016) Cancer treatment and survivorship statistics. *CA Cancer J Clin*, **66**: 271–89.
2. Xu M, Zhou L, Zheng L, *et al.* (2021) Sonodynamic therapy-derived multimodal synergistic cancer therapy. *Cancer Lett*, **497**: 229–42.
3. Shanei A and Akbari-Zadeh H (2019) Investigating the Sonodynamic-Radiosensitivity Effect of Gold Nanoparticles on HeLa Cervical Cancer Cells. *J Korean Med Sci*, **34**: 1–12.
4. Ebrahiminia A, Mokhtari-dizaji M, Toliyat T (2013) Ultrasonics Sonochemistry Correlation between iodide dosimetry and terephthalic acid dosimetry to evaluate the reactive radical production due to the acoustic cavitation activity. *Ultrason Sonochemistry*, **20**: 366–72.
5. Pan X, Bai L, Wang H, *et al.* (2018) Metal–organic-framework-derived carbon nanostructure augmented sonodynamic cancer therapy. *Adv Mater*, **30**: 1800180.
6. Samadian H, Hosseini-Nami S, Kamrava SK, *et al.* (2016) Folate-conjugated gold nanoparticle as a new nanoplatfrom for targeted cancer therapy. *J Cancer Res Clin Oncol*, **142**: 2217–29.
7. Mehrabi M, Esmailpour P, Akbarzadeh A, *et al.* (2016) Efficacy of pegylated liposomal etoposide nanoparticles on breast cancer cell lines. *Turkish J Med Sci*, **46**: 567–71.
8. Kosheleva OK, Lai T-C, Chen NG, *et al.* (2016) Selective killing of cancer cells by nanoparticle-assisted ultrasound. *J Nanobiotechnology*, **14**: 46.
9. Xu T, Zhao S, Lin C, *et al.* (2020) Recent advances in nanomaterials for sonodynamic therapy. *Nano Res*, **13**: 2898–908.
10. Heeran AB, Berrigan HP, O'Sullivan J (2019) The radiation-induced bystander effect (RIBE) and its connections with the hallmarks of cancer. *Radiat Res*, **192**: 668–79.
11. Mukherjee S and Chakraborty A (2019) Radiation-induced bystander phenomenon: insight and implications in radiotherapy. *Int J Radiat Biol*, **95**: 243–63.
12. Wang H, Yu KN, Hou J, *et al.* (2015) Radiation-induced bystander effect: early process and rapid assessment. *Cancer Lett*, **356**: 137–44.
13. Bilak A, Uyetake L, Su TT. (2014) Dying cells protect survivors from radiation-induced cell death in *Drosophila*. *PLoS Genet*, **10**: e1004220.
14. Widel M, Lalik A, Krzywon A, *et al.* (2015) The different radiation response and radiation-induced bystander effects in colorectal carcinoma cells differing in p53 status. *Mutat Res Mol Mech Mutagen*, **778**: 61–70.
15. Rezaei M, Kamran Samani R, Kazemi M, *et al.* (2021) Induction of a bystander effect after therapeutic ultrasound exposure in human melanoma: In-vitro assay. *Int J Radiat Res*, **19**: 183–9.
16. Marín A, Martín M, Liñán O, *et al.* (2015) Bystander effects and radiotherapy. *Reports Pract Oncol Radiother*, **20**: 12–21.
17. Bazak J, Korytowski W, Girotti AW (2019) Bystander effects of

- nitric oxide in cellular models of anti-tumor photodynamic therapy. *Cancers*, **11**: 1674.
18. Verma N and Tiku AB (2017) Significance and nature of bystander responses induced by various agents. *Mutat Res*, **773**: 104-21.
  19. Calatayud M, Asin L, Tres A, *et al.* (2015) Cell bystander effect induced by radiofrequency electromagnetic fields and magnetic nanoparticles. *Curr Nanosci*, **12**: 372-7.
  20. Daguene E, Louati S, Wozny A-S, *et al.* (2020) Radiation-induced bystander and abscopal effects: Important lessons from preclinical models. *Br J Cancer*, **123**: 339-48.
  21. Shanei A, Akbari-Zadeh H, Fakhimikabir H, *et al.* (2018) Evaluation of the therapeutic effect of 6-MV X-ray radiation on HeLa cells, in the presence of nanoparticles. *J Isfahan Med Sch*, **36**: 25-43.
  22. Shanei A, Akbari-Zadeh H, Fakhimikabir H, *et al.* (2019) The role of gold nanoparticles in sonosensitization of human cervical carcinoma cell line under ultrasound irradiation: An in vitro study. *J Nano Res*, **59**: 1-14.
  23. Sengupta S and Balla VK (2018) A review on the use of magnetic fields and ultrasound for non-invasive cancer treatment. *J Adv Res*, **14**: 97-111.
  24. Kooiman K, Roovers S, Langeveld SAG, *et al.* (2020) Ultrasound-responsive cavitation nuclei for therapy and drug delivery. *Ultrasound Med Biol*, **46**: 1296-325.
  25. Shanei A, Akbari-Zadeh H, Attaran N, *et al.* (2019) Effect of targeted gold nanoparticles size on acoustic cavitation: An in vitro study on melanoma cells. *Ultrasonics*, **102**: 106-120.
  26. Kosheleva OK, Lai P, Chen NG, *et al.* (2015) Nanoparticle-assisted ultrasound for cancer therapy. *Patent No.* 9,138,476.
  27. Brazzale C, Canaparo R, Racca L, *et al.* (2016) Enhanced selective sonosensitizing efficacy of ultrasound-based anticancer treatment by targeted gold nanoparticles. *Nanomedicine*, **11**: 3053-70.
  28. Rostami A, Toossi MTB, Szargania A, *et al.* (2016) The effect of glucose-coated gold nanoparticles on radiation bystander effect induced in MCF-7 and QUDB cell lines. *Radiat Environ Biophys*, **55**: 461-6.
  29. He L-L, Wang X, Wu X-X, *et al.* (2015) Protein damage and reactive oxygen species generation induced by the synergistic effects of ultrasound and methylene blue. *Spectrochim Acta Part A Mol Biomol Spectrosc*, **134**: 361-6.
  30. Yahyapour R, Motevaseli E, Rezaeyan A, *et al.* (2018) Mechanisms of radiation bystander and non-targeted effects: implications to radiation carcinogenesis and radiotherapy. *Curr Radiopharm*, **11**: 34-45.
  31. Ma Y, Zhang L, Rong S, *et al.* (2013) Relation between gastric cancer and protein oxidation, DNA damage, and lipid peroxidation. *Oxid Med Cell Longev*, **2013**, 1-6.
  32. Xu S, Wang J, Ding N, *et al.* (2015) Exosome-mediated microRNA transfer plays a role in radiation-induced bystander effect. *RNA Biol*, **12**: 1355-63.
  33. Bohari SPM, Aboulkheyr H, Nur ES, *et al.* (2017) Low intensity ultrasound induced apoptosis in MCF-7 breast cancer cell lines. *Sains Malays*, **46**: 575-81.
  34. Olsson MG, Nilsson EJC, Rutardóttir S, *et al.* (2010) Bystander cell death and stress response is inhibited by the radical scavenger  $\alpha$ 1-microglobulin in irradiated cell cultures. *Radiat Res*, **174**: 590-600.
  35. Koturbash I, Loree J, Kutanzi K, *et al.* (2008) In vivo bystander effect: cranial X-irradiation leads to elevated DNA damage, altered cellular proliferation and apoptosis, and increased p53 levels in shielded spleen. *Int J Radiat Oncol Biol Phys*, **70**: 554-62.
  36. Pae H-O, Oh G-S, Choi B-M, *et al.* (2004) Carbon monoxide produced by heme oxygenase-1 suppresses T cell proliferation via inhibition of IL-2 production. *J Immunol*, **172**: 4744-51.
  37. Fang J, Akaike T, Maeda H (2004) Antiapoptotic role of heme oxygenase (HO) and the potential of HO as a target in anticancer treatment. *Apoptosis*, **9**: 27-35.
  38. Bai W-K, Shen E, Hu B (2012) Induction of the apoptosis of cancer cell by sonodynamic therapy: a review. *Chinese J Cancer Res*, **24**: 368-73.
  39. Was H, Cichon T, Smolarczyk R, *et al.* (2006) Overexpression of heme oxygenase-1 in murine melanoma: increased proliferation and viability of tumor cells, decreased survival of mice. *Am J Pathol*, **169**: 2181-98.